Journal of Pharmaceutical Sciences 109 (2020) 730-738

Contents lists available at ScienceDirect

Journal of Pharmaceutical Sciences

journal homepage: www.jpharmsci.org

Pharmaceutical Biotechnology

Monoclonal Antibody Dimers Induced by Low pH, Heat, or Light Exposure Are Not Immunogenic Upon Subcutaneous Administration in a Mouse Model

Grzegorz Kijanka [1], Jared S. Bee [2], Mark A. Schenerman [2], Samuel A. Korman [2], Yuling Wu [3], Bram Slütter [1], Wim Jiskoot [1,*]

[1] Division of BioTherapeutics, Leiden University, Leiden, the Netherlands
[2] Analytical Sciences, MedImmune LLC, Gaithersburg, Maryland 20878
[3] Clinical Pharmacology and DMPK, MedImmune LLC, Gaithersburg, Maryland 20878

ARTICLE INFO

Article history:
Received 7 March 2019
Revised 12 April 2019
Accepted 18 April 2019
Available online 25 April 2019

Keywords:
immunogenicity
monoclonal antibody(s)
protein aggregation
immune response(s)
antibody drug(s)

ABSTRACT

The presence of protein aggregates is commonly believed to be an important risk factor for immunogenicity of therapeutic proteins. Among all types of aggregates, dimers are relatively abundant in most commercialized monoclonal antibody (mAb) products. The aim of this study was to investigate the immunogenicity of artificially created mAb dimers relative to that of unstressed and stressed mAb monomers. A monoclonal murine IgG1 (mIgG1) antibody was exposed to low pH, elevated temperature, or UV irradiation to induce dimerization. Dimers and monomers were purified via size-exclusion chromatography. Physicochemical analysis revealed that upon all stress conditions, new deamidation or oxidation or both of amino acids occurred. Nevertheless, the secondary and tertiary structures of all obtained dimers were similar to those of unstressed mIgG1. Isolated dimers were administered subcutaneously in Balb/c mice, and development of antidrug antibodies and accumulation of follicular T helper cells in draining lymph nodes and spleens were determined. None of the tested dimers or stressed monomers were found to be more immunogenic than the unstressed control in our mouse model. In conclusion, both dimers and monomers generated by using 3 different stress factors have a low immunogenicity similar to that of the unstressed monomers.

Introduction

Preservation of monoclonal antibody (mAb) structure during production, storage, and shipment is crucial for the efficacy and safety of mAb-based therapies. Because of their complex structure, proteins are generally more susceptible to degradation than small-molecule drugs. Despite extensive efforts undertaken to ensure the stability of mAb products, their degradation cannot be fully avoided. One of the most common mAb degradation products is aggregates.[1] Aggregation can be induced by multiple stress factors the product might be exposed to, such as pH shift, UV exposure, agitation, or elevated temperature.[2,3] Aggregates usually appear in a variety of sizes and structures, and their presence may have different biological consequences.[2-4] Multiple studies have shown that mAb aggregates increase the risk of antidrug antibody (ADA) formation, but the immunogenic potential differs for aggregates obtained via distinct stress conditions.[5-8] Formation of ADA may lead to altered bioavailability of the mAb and decreased efficacy and safety.[9,10] However, despite years of investigations, it still remains poorly understood how mAb aggregates may contribute to the ADA triggering and which feature, or set of features, determines whether aggregates will be immunogenic or not. A possible relation between aggregate size and immunogenicity has recently been investigated by several groups.[6,7,11-13] Depending on the study, the most immunogenic aggregates were found in the nanometer or micrometer range, but aggregate features other than size are most likely also important.[14]

Abbreviations used: Ab, antibody; ADA, antidrug antibody; Bis-ANS, 4,4′-dianilino-1,1′-binaphthyl-5,5′-disulfonic acid dipotassium salt; BSA, bovine serum albumin; CD, circular dichroism; HBS, histidine buffered saline; HRP, horse radish peroxidise; LN, lymph node; mAb, monoclonal antibody; MW, molecular weight; NTA, nanoparticle tracking analysis; MFI, micro-flow imaging; PBS, phosphate buffered saline; PBST, phosphate buffered saline with tween; PDI, polydispersity index; SC, subcutaneous; SDS-PAGE, sodium dodecyl sulfate–polyacrylamide gel electrophoresis; SEC, size-exclusion chromatography; Trp, tryptophan.
This article contains supplementary material available from the authors by request or via the Internet at https://doi.org/10.1016/j.xphs.2019.04.021.

* *Correspondence to:* Wim Jiskoot (Telephone: +31-71-527-4314).
E-mail address: w.jiskoot@lacdr.leidenuniv.nl (W. Jiskoot).

https://doi.org/10.1016/j.xphs.2019.04.021
0022-3549/

Until recently, low−molecular weight (MW) aggregates such as dimers have received less attention than submicron- and micron-size aggregates with respect to their possible immunogenicity. However, as the simplest mechanisms for bulk aggregation start with self-assembly of 2 monomers, one may expect dimers to be one of the most abundant aggregates in high-quality mAb products. Indeed, dimers are commonly found in commercially available mAb drugs.[15-17] Importantly, as mAbs are used in relatively high doses reaching hundreds of mg per injection,[1] even a small content of dimers in a formulation may result in a considerable dose (sometimes up to the mg range) of dimers being administered. Whereas the efficacy of treatment most likely will not be affected by the presence of a few percent of dimers in a formulation, the same cannot be assumed for immunogenicity. The impact of mAb dimers on immunogenicity has not been studied sufficiently. To our best knowledge, there is only one report published in which the immunogenicity of dimers was assessed.[6] The overall suggestion emerging from this article is that dimerization, if not accompanied by chemical modifications of mAb by UV-induced oxidation, does not increase the immunogenicity risk. However, further studies are necessary to investigate whether this finding holds true for different mAbs and types of dimers.

In our recent study, we showed that submicron-size aggregates of a monoclonal murine IgG1 (mIgG1) obtained by combination of low pH, elevated temperature, and stirring stresses were more immunogenic than oligomers and micron-size particles obtained under these stress conditions upon subcutaneous (SC) administration.[13] This aggregation protocol did not allow us to isolate stable dimers in quantities sufficient for *in vivo* testing. The aim of the present study was to investigate the immunogenicity of mIgG1 dimers upon SC administration in a mouse model. To induce dimerization, the mIgG1 was subjected to low pH or elevated temperature, that is, individual stress conditions from the protocol used in our previous study, or to UV irradiation. Dimers have been isolated via size-exclusion chromatography (SEC), thoroughly characterized and injected into Balb/c mice according to the treatment regimen used previously.[13] The immunogenicity was assessed by measuring follicular T cell accumulation in lymph nodes and spleens and by measuring the ADA response.

Material and Methods

Monoclonal Antibody

Recombinant murine IgG1 (pI: 6.8) formulated at 18.8 mg/mL in histidine buffered saline (HBS; 25 mM histidine, 150 mM NaCl, pH 6.0) was provided by MedImmune and used as a model mAb.

Generation and Fractionation of Dimers

Three distinct stress conditions were used to generate dimers. For the pH and temperature stresses, the mIgG1 was diluted with HBS supplemented with 5% sucrose to a concentration of 2 mg/mL. Aggregation-inducing experiments were performed in 1.5-mL Eppendorf tubes, with 0.4 mL of mIgG1 solution per tube. The pH stress was induced by adding 1 M HCl to obtain a pH of 2.5 and leaving the acidified sample at ambient temperature for 1 h. After bringing the pH back to 6 with 1 M NaOH, 20 tubes of stressed mIgG1 were pooled and the total volume of the solution was reduced to ca. 1 mL by using a VivaSpin® centrifugal concentrator (Sartorius Stedim Biotech GmbH, Goettingen, Germany). For the temperature stress, 1.5-mL Eppendorf tubes containing 0.4 mL of mIgG1 solution per tube were incubated at 65°C for 10 min in an Eppendorf Thermomixer (Eppendorf, Hamburg, Germany). Next, the tubes were cooled down at 4°C for 10 min and the content of 48 tubes was pooled for volume reduction as described previously. For the UV stress, 3 mL of the undiluted mIgG1 in a 3-mL Schott FIOLAX drug vial (Schott AC, Mainz, Germany) was exposed to UV-VIS light (irradiance energy 10.68 W/m^2) for 96 h in a light chamber (Powers Scientific Inc., Warminster, PA) at 23°C. The fractionation of pH- and temperature-stressed samples was performed directly after stressing. The UV-stressed material was aliquoted into 1.5-mL vials, 1 mL per vial, and stored at −80°C before being processed.

The dimers and monomers subjected to stress conditions were isolated via SEC on an Agilent 1200 system (Agilent Technologies, Palo Alto, CA) equipped with an autoinjector and a fraction collector. Fractions were separated on a HiLoad Superdex 200 PG column (GE Healthcare, Buckinghamshire, UK). Before fractionation the stressed protein solutions were centrifuged at 18,000× *g* at 4°C for 10 min. Next, 0.9 mL of supernatant was injected onto the column, HBS was used as mobile phase, and the flow rate was 1 mL/min. One-millilitre fractions were collected between 45 and 75 min of separation, and fractions containing dimers and monomers were identified on the basis of absorbance at 280 nm and pooled (see Supplementary Fig. S1). The 3 different dimer-enriched products obtained are referred to as "pH dimer," "Temp dimer," and "UV dimer." Monomers subjected to stress conditions and purified with SEC are referred to as "pH monomer," "Temp monomer," and "UV monomer." On fractionation, all isolated samples were stored at −80°C before use. After thawing, the samples were centrifuged at 18,000× *g*, 4°C for 30 min to remove submicron- and micron-size particles that might have been formed during this freeze-thawing cycle.

The positive control, referred to as "supernatant," containing mainly submicron-size particles, was prepared freshly before each injection as described previously by Kijanka et al.[13] (see Supplementary Figs. S2 and S3 for details about the supernatant composition).

The protein concentration of all dimeric and monomeric species was calculated from the area under the respective peaks obtained during the SEC analysis described in Section Characterization of Dimers. Samples were screened for endotoxin contamination with the Pierce® LAL Chromogenic Endotoxin Quantitation Kit according to the manufacturer's protocol (Thermo Fisher Scientific, Rockford, IL). The measured endotoxin levels were below 0.02 EU/injected dose, which is below the endotoxin limit for injectable solutions of 5 EU/kg/h given in United States Pharmacopeia <85> chapter.[18]

Characterization of Dimers

High-Performance Size-Exclusion Chromatography

SEC was used to quantify the content of monomers, dimers, and oligomers in isolated fractions. Ten microliter of each sample was analyzed on an Agilent 1200 system (Agilent Technologies) equipped with an autoinjector, an absorbance detector, and a multiangle laser light scattering Dawn Helios detector (Wyatt Technology, Dernbach, Germany). A MabPac SEC-1 column (Thermo Fisher Scientific, Rockford, IL) was used for separation with HBS as an eluent. Samples were separated for 20 min at a flow rate of 0.2 mL/min. The protein peaks were detected at 280 nm, and the MW of the eluting material was calculated on the basis of multiangle laser light scattering data in the Astra V 5.3.4.20 software (Wyatt Technology).

Dynamic Light Scattering

Malvern Zetasizer Nano ZS (Malvern, Herrenberg, Germany) equipped with a 633-nm He-Ne laser operating at an angle of 173° was used for dynamic light scattering analysis. A 100 μL of each fraction in a polystyrene micro cuvette (Brand, Wertheim, Germany) with a 10-mm path length was analyzed at 25°C with an automatic attenuation, run duration, and number of runs. Data

were collected with the Zetasizer Software v.7.11 (Malvern). The mean Z-average diameter (Z_{ave}) and polydispersity index (PDI) of 4 representative dimer batches are reported.

Nanoparticle Tracking Analysis

Submicron size particles (size range 0.1 μm-1 μm) in all isolated samples were counted and sized with a NanoSight LM20 (NanoSight, Amesbury, United Kingdom), equipped with a sample chamber with a 640-nm laser and a syringe pump. Before analysis all samples were diluted 10 fold in HBS. The measurement was performed for 90 s with manual adjustment of shutter and gain. Each sample was measured 3 times. The data was acquired and analyzed by the NTA 2.3 software (NanoSight). The data for all 8 batches of dimers used for injections are reported.

Micro-Flow Imaging

The number of micron-size particles (size range 1 μm-100 μm) was determined by using an micro-flow imaging (MFI) DPA4100 series A system (ProteinSimple, Santa Clara, CA) operating at high magnification (14×). A silane-coated 100-μm flow cell (ProteinSimple) was used for all measurements. A sample (10-fold diluted with HBS) of 0.2 mL was analyzed at a flow rate of 0.17 mL/min. Each measurement was performed in duplicate. Data were acquired by the MFI View software, version 6.9, and analyzed with MVAS, version 1.2, (ProteinSimple). The data for all 8 batches of dimers used for injections are reported.

Sodium Dodecyl Sulfate Polyacrylamide Gel Electrophoresis

One microgram of protein from each fraction was separated on 4%-15% Mini-Protean® TGX™ pre-cast gel (Bio-Rad Laboratories B.V., Veenendaal, The Netherlands). A Laemmli sample buffer (Bio-Rad Laboratories B.V.) with or without a β-mercaptoethanol (Bio-Rad Laboratories B.V.; final concentration 355 mM) was used. Samples were incubated at 95°C for 5 min before loading on the gel. The electrophoresis was performed with a Bio-Rad Mini-Protean module and 25 mM Tris, 192 mM glycine, 0.1% sodium dodecyl sulfate, pH 8.3 (Bio-Rad Laboratories B.V.) as a running buffer. Separation was initiated with electrophoresis at 80 V for 10 min, followed by 120 V for 50 min. The MW was estimated on the basis of Spectra™ Multicolor High-Range Protein Ladder (Thermo Fisher Scientific) and Precision Plus Protein™ All Blue Standards (Bio-Rad Laboratories B.V.). Bands were visualized with a Silver Stain Plus kit (Bio-Rad Laboratories B.V.) according to manufacturer's protocol. The images of gels were acquired with a GS-900 densitometer (Bio-Rad Laboratories B.V.) and the Image Lab v.5.2.1 software (Bio-Rad Laboratories B.V.). The Image Lab software was also used for band analysis and calculation of percentage of covalent dimers in the injection solutions.

Western Blotting and Dot Blotting

For Western blot analysis, 0.1 μg of protein of each fraction was separated by sodium dodecyl sulfate–polyacrylamide gel electrophoresis (SDS-PAGE) under nonreducing conditions as described previously. Next, SDS-PAGE gels were blotted onto a supported nitrocellulose sheet (Bio-Rad Laboratories B.V.) with a Bio-Rad Mini Trans-Blot electrophoretic transfer cell and 25 mM Tris, 192 mM glycine and 20% methanol, pH 8.3 as a running buffer. Membranes were blocked overnight at 4°C with 2% bovine serum albumin (BSA) in phosphate buffered saline (PBS) supplemented with 0.05% Tween 20 (PBST). Next, the blots were incubated for 1 h at ambient temperature with horse radish peroxidase (HRP)–labeled anti-mouse total IgG, IgG1, IgG2a (Southern Biotech, Birmingham, AL), or specific anti-mIgG1 polyclonal antibody purified from sera of rabbits immunized with mIgG1 by Covance (Denver, CO), all diluted 2000-fold in PBST. Then, the membranes incubated with HRP-Abs were washed 3 times with PBST, followed by 2 PBS washes, and developed with 3-amino-9-ethylcarbazole chromogenic substrate (Sigma-Aldrich Chemie B.V., Zwijndrecht, The Netherlands) according to the manufacturer's protocol. The membrane incubated with rabbit anti-mIgG1 was washed 3 times with PBST and then incubated for 1 h with peroxidase-labeled anti-rabbit Ab (Thermo Fisher Scientific), diluted 2000-fold in PBST. Finally, the membrane was washed and developed with 3-amino-9-ethylcarbazole chromogenic substrate.

Far-UV Circular Dichroism Spectroscopy

For far-UV circular dichroism (far-UV CD), samples in HBS were buffer-exchanged into 10 mM phosphate buffer, pH 7.2 with dialysis using 0.5-3 mL Slide-a-Lyzer™ dialysis cassettes (Thermo Fisher Scientific, Rockford, USA). Next, the protein concentration of all mIgG1 samples was adjusted to 0.1 mg/mL according to their absorbance at 280 nm. The CD spectra were collected with a Jasco J-815 CD spectrometer (Jasco International, Tokyo, Japan) at 25°C. A quartz cuvette with a path length of 0.2 cm was used. The CD spectra were collected from 190 nm to 250 nm at a speed of 100 nm/min, a data pitch of 0.2 nm, a response time of 8 s, and a bandwidth of 1 nm. For each sample, 5 accumulations were collected. Acquired spectra were smoothed with GraphPad Prism® v 5.02 (GraphPad Software, Inc., La Jolla, CA) as described previously[13,19] and background corrected for the baseline spectrum of phosphate buffer. A mean residue ellipticity ([θ] mean residue weight [MRW]) was calculated according to Kelly et al.,[20] using a MRW of 112.35 (MRW = M/N − 1, where M is a molecular mass, i.e., 148300 Da, and N is the number of amino acid residues of mIgG1, i.e., 1320).

Fluorescence Spectroscopy

The fluorescence emission spectra of isolated fractions were measured with a steady-state fluorimeter FS900 (Edinburgh Instruments Ltd., Livingston, UK) equipped with a plate reader. All measurements were performed on 96-well, black, flat-bottom, polystyrene plates (Greiner Bio One, Alphen aan den Rijn, the Netherlands). A volume of 200 μL of each 0.1 mg/mL sample was used. The intrinsic tryptophan (Trp) fluorescence was recorded from 310 to 400 nm on excitation at 295 nm. The slits of 3 nm, a dwell time of 1 s, and steps of 0.5 nm were used. The final spectrum was obtained by a cumulative addition of 3 scans. All spectra were first smoothed as described previously, and then background corrected for the spectrum of the HBS.

Next, 4,4′-dianilino-1,1′-binaphthyl-5,5′-disulfonic acid dipotassium salt (Bis-ANS; Sigma-Aldrich B.V.) was added to each fraction to a final concentration of 1 μM. The Bis-ANS was excited at 385 nm, and the fluorescence emission was recorded from 410 nm to 600 nm with 1-nm steps and a dwell time of 1 s. The excitation and emission slits were both set to 5 nm, and a cumulative addition of 3 scans for each spectrum was collected. The obtained spectra were smoothed, and buffer corrected as described previously.

Tryptic Peptide Mapping Using Liquid Chromatography Coupled With Mass Spectrometry

Potential post-translational modifications and stress-induced chemical degradation were assessed by tryptic digest peptide mapping of all samples used in the animal experiments. Denaturation and reduction of 100 μg protein (100 μL protein samples at 1 μg/μL) were initiated by addition of 200 μL of 8 M guanidine, 130 mM Tris, 1 mM EDTA, pH 7.6, and 10 μL of 500 mM dithiothreitol (Thermo Fisher Scientific). Next, the samples were incubated at 37°C for 30 min. The samples were then alkylated with the addition of 25 μL of 500 mM iodoacetamide (G-Biosciences, St. Louis, MO) and incubation at ambient temperature for 30 min while protected

from light. Finally, samples were buffer-exchanged into 2 M urea, 100 mM Tris, pH 7.6 by centrifugal filtration with a 10-kDa MW membrane (Millipore Sigma, St. Louis, MO) and digested at 37°C for 4 h by using 5 μg of trypsin. The reaction was quenched with 4% trifluoroacetic acid, and samples were collected for analysis.

Peptides were separated on a Waters Acquity UPLC system with an autosampler and tunable UV detector (Waters Corporation, Milford, MA) equipped with a BEH300 C18 column (1.7 μm, 2.1 × 150 mm; Waters Corporation). Peptides were eluted from the column by using a gradient from 100% to 65% mobile phase A (0.02% TFA in water, mobile phase B was 0.02% TFA/acetonitrile) at a flow rate of 0.2 mL/min and total elution time of 78 min. Eluted peptides were detected by UV absorbance at 220 nm and analyzed by a Waters Synapt G2 QTOF mass spectrometer (Waters Corporation). Data were acquired and analyzed using the Waters UNIFI and MassLynx software (Waters Corporation).

Estimation of Protein Mass Within Different Size Ranges of Aggregates

SEC, nanoparticle tracking analysis (NTA), and MFI were used to estimate the mass of protein in different size ranges for each enriched fraction as described previously.[13,21-23] In short, the mass of mIgG1 fragments, monomers, and oligomers was calculated from the peak areas under the curve in the SEC analysis. The mass of protein submicron- and micron-size particles was calculated on the basis of NTA and MFI data according to the formula proposed by Barnard et al., that is, $M = d*V*n*p$, where d is the density of the protein (1.4 mg/mL), V is the volume of particles per size bin (1 nm for NTA and 0.25 μm MFI), n is the number of particles per size bin, and p is the fraction of the particle volume (V) occupied by protein (assumed to be 0.75).[21]

Animal Study

Mice

BALB/c mice aged 6-8 weeks were obtained from Charles River Laboratory (L'Arbresle Cedex, France) and kept in standard cages with access to food and water (acidified) *ad libitum*. All testing was conducted with approval of the Animal Ethic Committee of Leiden University Medical Center (protocol number 14096).

Animal Experiments

A total number of 128 mice were divided into 8 groups ($n = 16$) of which 3 were treated with different dimer-enriched fractions, 3 with the corresponding stressed monomers, one with unstressed mIgG1 (referred to as "unstressed") as a negative control, and one with supernatant (positive control). Mice were injected subcutaneously between the shoulders, twice per week for 8 weeks with 10 μg of protein diluted in endotoxin-free HBS. The basal level of ADA was determined for each mouse in blood collected from the submandibular vein before the first injection. From each mouse, blood was collected every second week. Four mice per group were sacrificed 1 week after the second injection (day 10 of the experiment), and the remaining animals were sacrificed 2 weeks after the last injection (day 65). The draining lymph nodes (LNs), that is, brachial and axillary LNs, and spleens were extracted after euthanasia for *ex vivo* analysis.

Blood was collected into the MiniCollect® Serum Z separator tubes (Greiner Bio-One). Serum was isolated by centrifugation (3000× *g*, 10 min, 4°C), collected into storage tubes (Thermo Fisher Scientific), and kept at −80°C for analysis.

Antidrug Antibody Detection

The ADA screening was performed with a bridging ELISA as described previously.[13,24] A biotinylated and digoxigeninylated mIgG1 were used as capture and detection reagents, respectively. Dulbecco's PBS (Thermo Fisher Scientific) supplemented with 0.5% BSA (Sigma-Aldrich Chemie B.V.) was used as assay buffer, and polyclonal rabbit anti-mIgG1 antibody was used as the assay-positive control. Between detection steps, plates were washed 8 times with PBST. Samples and polyclonal rabbit anti-mIgG1 ADA assay controls (spiked in pooled BALB/c sera) were diluted at a minimum dilution of 1/100 in assay buffer and incubated overnight with capture and detection reagents (1.25 μg/mL each). On the following day, samples were transferred into wells of a streptavidin-coated plate (Thermo Fisher Scientific) and incubated at room temperature for 1 h to capture the ADA-bridged complexes. After a wash, a peroxidase-labeled anti-digoxigenin antibody (Jackson Immunolabs, Suffolk, UK) was added into the wells and the resulting mixtures were incubated for 1 h and washed away. The QuantaRed™ Enhanced Chemifluorescent was used as the HRP Substrate Kit (Thermo Fisher Scientific). The fluorescence was excited at 570 nm, and emission at 585 nm was measured with a Tecan Infinity plate reader (Tecan Group Ltd., Männedorf, Switzerland).

The signal of each sample was normalized against background signal for pooled negative BALB/c sera (Bioreclamation, Westbury, NY). A cutoff point was defined as the upper 95th percentile of the signal-to-background ratios (S/B's) from basal blood samples ($n = 84$). Serum was classified as positive if the S/B was equal to or higher than the cutoff point. All samples found to be positive in the screening assay were tested in a confirmatory assay in which the unlabeled mIgG1 was used as a competitor during the overnight incubation step.[13]

Follicular T Helper Cell Detection

A single cell suspension was prepared by pressing spleens and LNs through a Falcon® 70-μm cell strainer (Corning, Amsterdam, The Netherlands). Next, red blood cells present in splenocytes after the suspension were lysed with ACK lysis buffer (Thermo Fisher Scientific) according to manufacturer's protocol. Approximately 100,000 cells were suspended in 100 μL of cold PBS with 1% BSA and stained on ice with anti-CD3-FITC, CD4-eFluor450, CXCR5-PeCy7, and PD1-PE Abs (all eBioscience, Vienna, Austria), diluted according to manufacturer's protocol. After 40-min incubation, cells were spun down (300 g) and unbound detecting reagents were removed by 2 times washing with PBS with 1% BSA. After the last wash, cells were fixed with 1% polyformaldehyde in PBS and analyzed with a FACS Canto II flow cytometer (BD Biosciences, Vianen, The Netherlands). The obtained data were analyzed with FlowJo® X (FlowJo LLC, Ashland, OR) using the gating strategy described previously to quantify follicular T helper (T_{FH}) cells.[13]

Statistical Analysis

The potential difference between ADA responses upon injection of different fractions was assessed with one-way ANOVA with Dunnet's multiple comparison test. Calculations were performed in the GraphPad Prism® v.5.02 software.

Results

Composition of Fractions Enriched in Dimers

The mass of mIgG1 in the form of monomers, dimers, or larger aggregates was estimated on the basis of SEC, NTA, and MFI data (Fig. 1). The composition of all dimeric fractions and the corresponding monomeric counterparts is shown in Figure 2. All dimer-enriched fractions were composed of at least 50% dimers. The highest dimer content (85%) was found in UV dimers, followed by

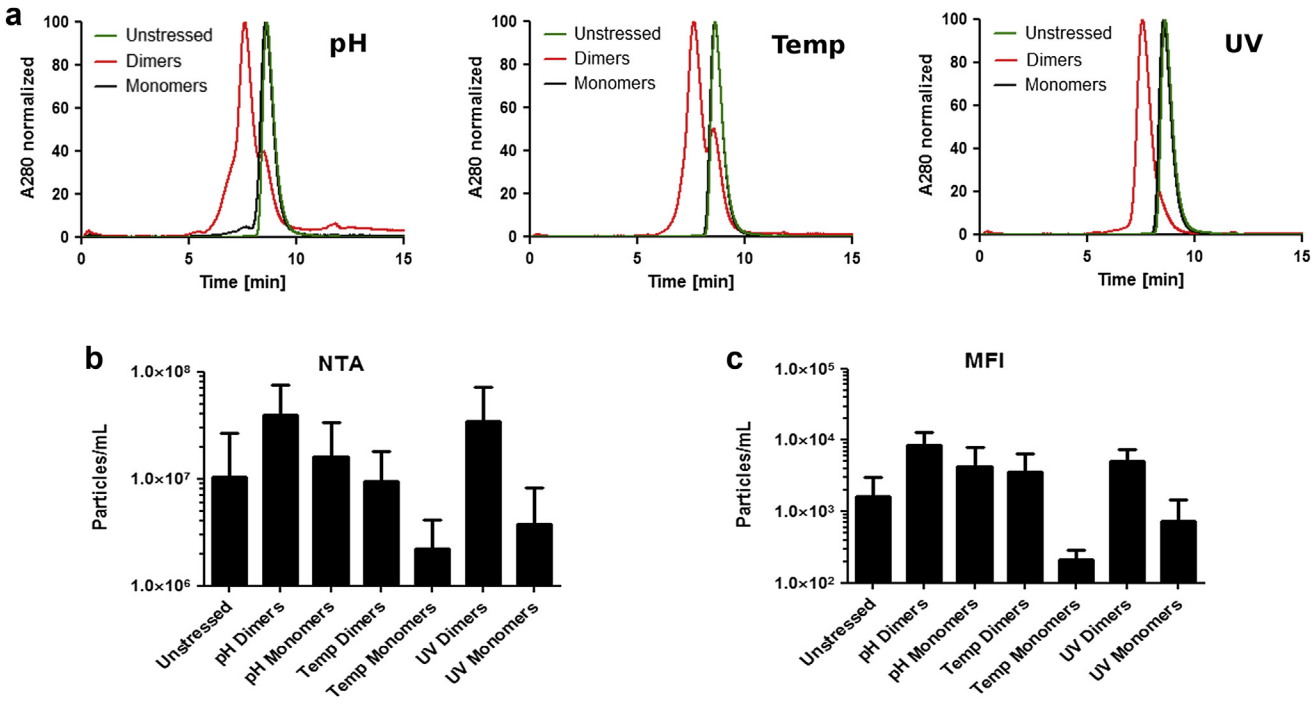

Figure 1. Size distribution of the samples used for immunogenicity assessment. (a) Representative SEC chromatograms recorded at A_{280}. (b) Average concentrations of submicron-size (NTA) particles. (c) Average concentrations of micron-size (MFI) particles. The bars represent the average values (+SD) for 8 batches of each sample.

Temp dimers and pH dimers (56% and 54%, respectively). All these fractions contained also significant amounts of monomers, ranging from 13% in UV dimers to 40% in Temp dimers. Oligomers accounted for 14% of pH dimers, 4% of Temp dimers, and 1.9% of UV dimers. The amount of submicron- and micron-size particles in all dimer samples was negligible (all estimated to be below 1.5%). Unstressed control and all fractions containing stressed monomers were indeed composed of mainly monomers (>96%). Only pH monomers contained a small amount of dimers (ca. 3%). In contrast, the supernatant primarily consisted of submicron-size particles with small amounts of oligomers and micron-size particles (see Supplementary Fig. S2).

According to the dynamic light scattering analysis, the Z_{ave} of Temp monomers and UV monomers was highly similar to that of

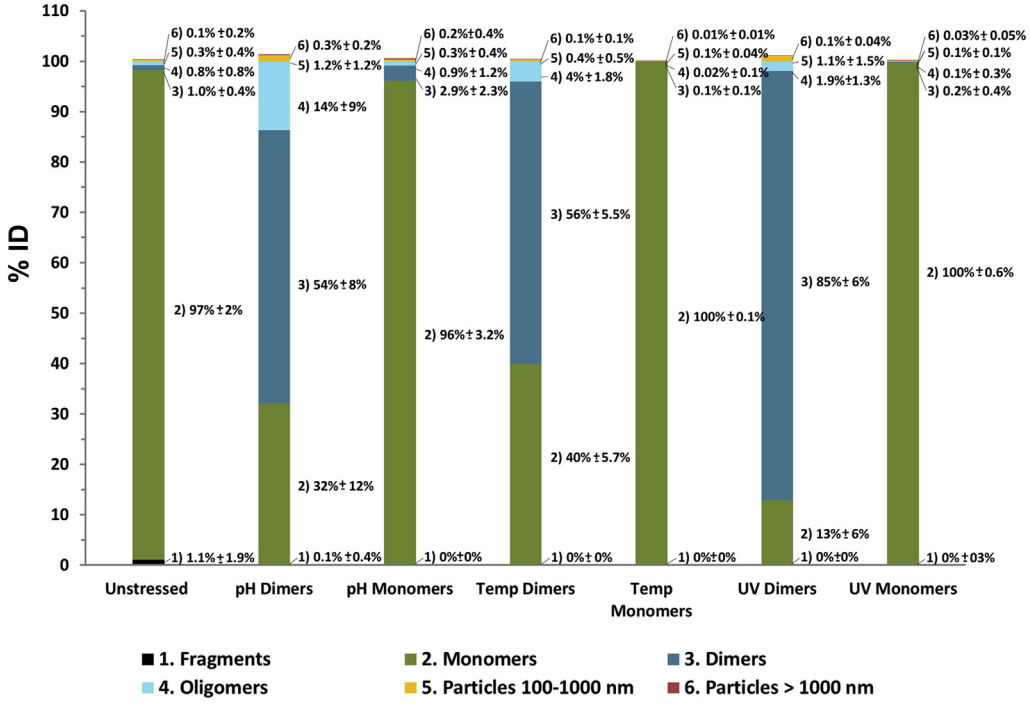

Figure 2. Composition of injected samples expressed as a percentage of injected dose (%ID) calculated on the basis of SEC, NTA, and MFI.

Table 1
Summary of the Results of Dynamic Light Scattering Measurements (Average ± SD; $n = 4$ Batches)

Sample	Dynamic Light Scattering	
	Z_{ave} (nm)	PDI
Unstressed	11.7 ± 0.8	0.09 ± 0.06
pH Monomer	14.0 ± 1.1	0.23 ± 0.04
pH Dimer	20.5 ± 3.8	0.20 ± 0.04
Temp Monomer	11.3 ± 0.3	0.06 ± 0.04
Temp Dimer	21.3 ± 5.3	0.24 ± 0.07
UV Monomer	11.4 ± 0.2	0.08 ± 0.02
UV Dimer	22.9 ± 4.2	0.24 ± 0.04

unstressed mIgG1 (ca. 11.5 nm, see Table 1). The measured Z_{ave} of pH monomers was slightly larger, 14 nm, probably due to the small amount of dimer in the pH monomer fraction or the presence of expanded monomers or both, as has been observed before for pH-stressed IgG.[19] The Z_{ave} of all dimer-enriched fractions was very similar (20-23 nm). It has to be noted that the PDI of unstressed, Temp monomers, and UV monomers was below 0.1, indicating highly homogenous composition of these fractions. The PDI of all other solutions was within the range of 0.2-0.25.

Structural Characterization

The secondary structure of the mIgG1 in the different samples was assessed by far-UV CD spectroscopy. As depicted in Figure 3, only minor alterations in the far-UV CD spectra when compared with unstressed control were observed, indicating that the mIgG1 secondary structure was highly preserved after stress treatment and fractionation of dimers and monomers. All spectra are typical for IgG1 dominated by beta-sheet.[20,25,26]

Possible alteration in tertiary structures was determined by measurement of intrinsic Trp fluorescence (Fig. 3). The spectra of pH- and temperature-stressed samples were very similar to the spectrum of unstressed control. However, a minor shift in the emission wavelength maximum (λ_{max}) from 346 nm for unstressed control to 347.5 nm for pH dimers and 347 nm for Temp dimers was recorded. The λ_{max} of pH monomers was 346.5 nm, and for Temp monomers, 346 nm. In contrast, the fluorescence intensity of UV-treated samples was almost 2 times lower than that of unstressed control. The shift in λ_{max} for both UV dimers and UV monomers was minimal (λ_{max} of 346.5 nm and 345.5 nm, respectively).

Additional assessment of possible alteration in tertiary structures was done by adding extrinsic, hydrophobic probe (Bis-ANS) to all fractions and measuring its fluorescence. As shown in Figure 3, the fluorescence of Bis-ANS in the presence of Unstressed control, UV dimers, and all monomeric samples was similarly low, indicating lack of exposure of new hydrophobic patches on the mIgG1 surface after applying stress and fractionation. In contrast, in the presence of pH dimers and Temp dimers, the Bis-ANS fluorescence was elevated.

In addition to spectrofluorometric measurements, all fractions were analyzed with SDS-PAGE and Western blotting (Fig. 4). SDS-PAGE revealed that 58% of all dimers found in UV dimers and 38%

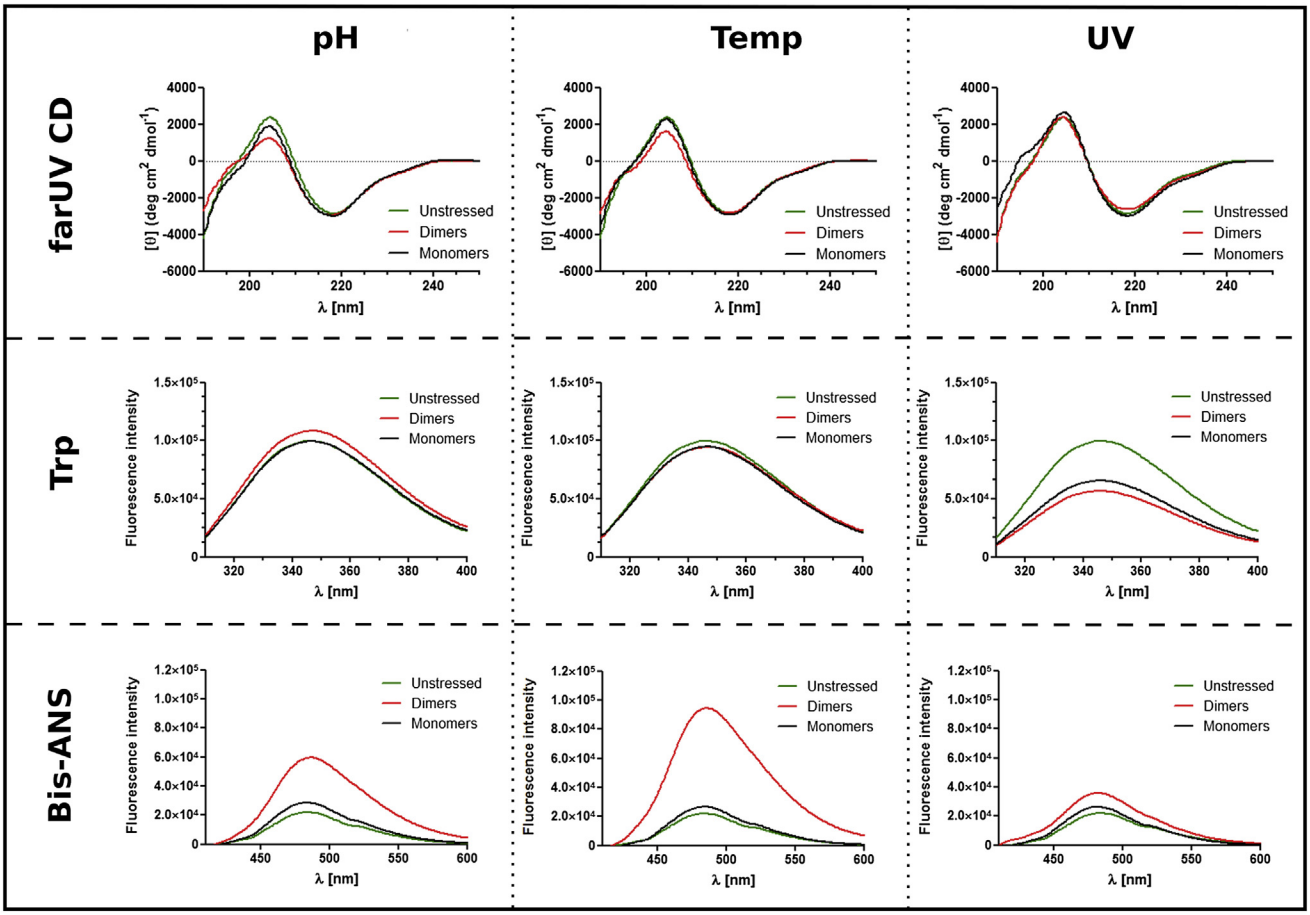

Figure 3. Spectra resulting from structural characterization of mIgG1 samples with far-UV CD (upper panels), intrinsic Trp fluorescence (middle plots), and extrinsic Bis-ANS fluorescence (lower plots). Each spectrum is an average of 3 independent experiments.

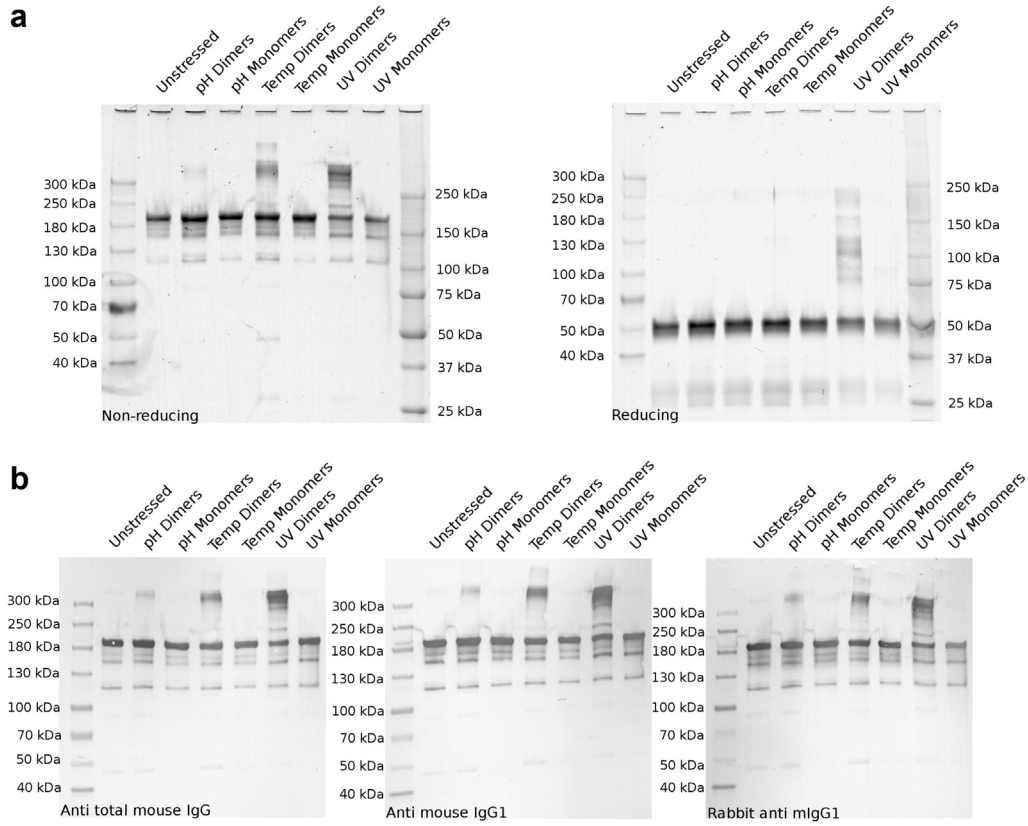

Figure 4. SDS-PAGE (a) and Western blot (b) analysis of injection solutions.

in Temp dimers were covalently bound. In contrast, the vast majority of the dimers in pH dimers were not covalent (only 7.6% of the dimers were covalently linked). On treatment with reducing agent, all dimers in pH dimers and Temp dimers were dissociated, indicating that these dimers were mediated by disulfide bridge formation. In UV dimers, several bands with apparent MWs higher than 50 kDa, that is, mAb's heavy chain weight, were detected, pointing to other chemical modifications besides disulfide bridges.

In Western blot analysis, all species of all samples, both monomeric and dimeric, were recognized by a panel of polyclonal antibodies used for mIgG1 detection, similarly to unstressed control, indicating the preservation of native epitopes in the stressed samples (Fig. 4b).

Liquid Chromatography Coupled with Mass Spectrometry

Tryptic peptide mapping by liquid chromatography coupled with mass spectrometry analysis revealed that all stress conditions applied to induced dimers resulted in some chemical modifications of both monomer and dimer fractions. Unstressed mIgG1 contained low levels of oxidized and deamidated amino acid residues in the heavy chain (Table 2). The pH stress not only increased the level of existing deamidation sites but also led to deamidation of asparagine 74 and 84. In contrast, UV stress did not change deamidation levels but increased the level of oxidation and led to new oxidation sites in both heavy (Trp 47 and 110) and light chains (Trp 37 and methionine 49). Temperature treatment led to increased oxidation and deamidation at existing and new sites.

Immunogenicity

The immunogenicity of the different dimers and their stressed monomeric counterparts was assessed by detecting ADA in blood and determination of T_{FH} cells activation in LNs and spleens. Administration of stressed monomers or dimers did not trigger ADA formation in any of the mice, similarly to unstressed control, throughout the entire time course of the experiment. Figure 5a shows the results for the last time point (day 65). Moreover, no significant change in the number of T_{FH} cells in LNs or spleens at any time point of treatment was detected (Fig. 5b and Supplementary Fig. S4). In contrast to dimer-enriched samples, the supernatant triggered ADA in 5 of 12 mice, in line with our previous publication.[13] Moreover, the number of T_{FH} cells in spleens extracted on day 65 from mice treated with supernatant was significantly higher than in mice receiving unstressed control ($p < 0.05$).

Discussion

By definition, an aggregate is an assembly of protein molecules of MW higher than that of the physiologically active unit. For IgGs, the smallest possible aggregate is a dimer, that is, an assembly of 2 IgG molecules. Naturally occurring dimers of IgG1 and IgG2 subtypes have been found in serum.[27] Moreover, dimers have been identified in several commercial mAb products.[15-17] Despite their small size, dimers display diverse characteristics, as demonstrated in several studies. In a study by Remmele et al., dimers of eprazumab, a humanized IgG1, were found to be mostly covalent, biologically active, and with a highly preserved mAb secondary structure. The dimerization was found to be facilitated via Fab:Fab, Fc:Fc, and Fab:Fc interactions.[15] Similarly, dimers of another humanized IgG1, palivizumab, were also found to be partially covalent, fully active and of native structure.[16] However, in contrast to the eprazumab study, only interactions between Fab:Fab and Fab:Fc were identified. In another report describing structural characterization of dimers, Paul et al. compared artificially created and

Table 2
Results of Peptide Mapping With Liquid Chromatography Coupled With Mass Spectrometry Analysis of the mIgG1 Fractions

Sample	% Peak Area					
	Oxidation					
	Heavy Chain				Light Chain	
	M34, W36	W47	W110	M255	W37	M49
Unstressed	0.9	ND	ND	1.1	ND	ND
pH Monomers	2.1	ND	ND	1.5	ND	ND
pH Dimers	1.9	ND	ND	1.7	ND	ND
Temp Monomers	5.1	ND	1.6	6.4	ND	3.7
Temp Dimers	4.8	ND	2.1	6.1	ND	4.1
UV Monomers	4.3	2.0	1.8	2.8	2.4	1.0
UV Dimers	4.0	2.2	2.3	3.0	1.9	0.9

Sample	Deamidation					Isomerization	
	Heavy Chain					Heavy Chain	
	N52N53N54(G)	N74(S)	N84(S)	Q112(G)	N387(G)N392N393(Y)	D62(S)	D108(S)
Unstressed	1.3	ND	ND	ND	5.1	ND	ND
pH Monomers	4.0	1.1	1.4	ND	8.6	ND	ND
pH Dimers	5.2	1.1	1.1	ND	7.9	ND	ND
Temp Monomers	4.1	1.8	1.5	ND	6.0	ND	ND
Temp Dimers	3.7	1.5	1.6	ND	6.3	ND	ND
UV Monomers	2.0	ND	ND	ND	4.5	ND	ND
UV Dimers	2.1	ND	ND	ND	4.0	ND	ND

ND, not detected.

"process-related" dimers of IgG1.[28] For dimers obtained via process-related stress or UV irradiation, interactions between Fab:Fab were identified. In contrast, pH stress led to formation of dimers via Fab:Fab or Fab:Fc bonds. All dimers differed in potency and Fc receptor binding affinity. The potency of pH dimers was similar to that of unstressed control, but the potency of UV and process-related dimers was strongly reduced. All dimers showed increased affinity to an Fc receptor. In another study, dimers of 3 humanized IgG1s were investigated.[29] All tested IgG1s tended to form predominantly 2 distinct forms of dimers, referred to as "compressed" and "elongated" types. Both forms of dimers were formed exclusively via Fab:Fab interactions. The binding between 2 antigen binding sites resulted in an elongated, fiber-like form of dimer. Both covalent and noncovalent links were identified in this type of dimers. In contrast, the compressed, globular dimers were created by noncovalent interaction of constant regions of Fab domains or hinge regions.

The result of physicochemical characterization of dimers used in this study is in accordance with observations described in the literature. Mainly noncovalent pH dimers and mostly covalent UV dimers have been described for another mAb.[28] Also, covalent, nonreducible bonds have been previously observed for UV-treated mAbs.[5,28] Moreover, the observation that dimerization did not measurably affect the secondary structure of mIgG1, even when accompanied by chemical modifications, corresponds with the results of Paul et al.[28] In our present study, the analysis of intrinsic Trp fluorescence suggested no major alterations in tertiary structure of all dimer types. Lower maximum fluorescence of Trp in UV-stressed samples originated most likely from its oxidation (leading to a decreased number of intact Trp residues) rather than from changes in Trp's local environment.[30] This is in line with the lack of increase of Bis-ANS fluorescence in presence of UV dimers. Interestingly, despite the apparent high level of preservation of secondary and tertiary structures for pH dimers and Temp dimers, the Bis-ANS fluorescence in presence of these solutions was elevated. This observation might indicate that some hydrophobic patches on pH dimers and Temp dimers have been exposed during dimerization. However, it cannot be excluded that increased Bis-ANS fluorescence in presence of pH dimers and Temp dimers was due to oligomers that were co-purified with these dimers (14% of pH

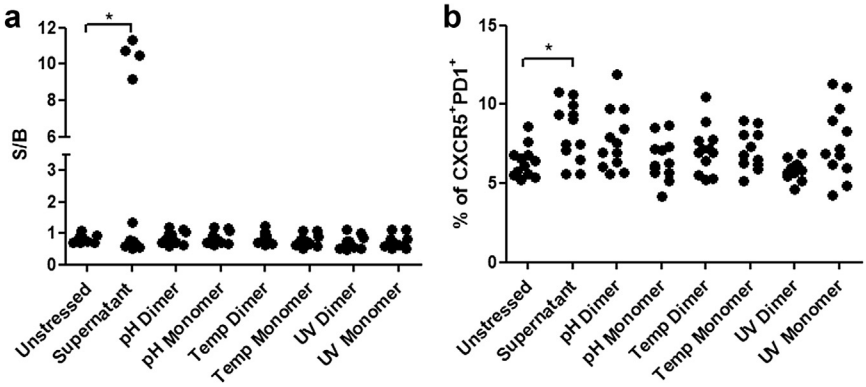

Figure 5. *In vivo* assessment of immunogenic potential of dimer-enriched samples. (a) ADA production. (b) Activation of T_{FH} in spleen. Both measurements were performed 2 weeks after the last mIgG1 administration (day 65). Each dot represents the result for individual mouse. $^{*}p < 0.05$.

dimer and 4% of Temp dimer according to SEC). The SEC chromatograms of crude pH and temperature-stressed mIgG1 show that, in contrast to UV irradiation, significant amount of trimers and higher-MW oligomers have been created during aggregation (see Fig. S1). The increase in Bis-ANS fluorescence suggests that these oligomers might contain conformationally altered mIgG1 similarly to submicron-size particles found in supernatant (see Supplementary Fig. S3).

There is very limited data available regarding the relation between dimerization of mAb and potentially increased risk of immunogenicity. To our best knowledge there is only one manuscript available tackling the problem of immunogenicity of dimers. Bessa et al.[6] investigated the relation between human IgG1 aggregate size (up to oligomers) and immunogenicity. In this study aggregates were induced by low pH, UV exposure and "process related" stresses and separated into fractions enriched in monomers, dimers and higher-MW oligomers. Among all tested dimers, only UV-irradiated ones induced higher ADA levels than unstressed monomeric control in transgenic mice. These data led to the conclusion that a combination of aggregation and chemical modifications is required for ADA formation. Our data partially correspond with this report, as none of the tested dimers, even those carrying higher levels of post-translational modifications than unstressed control, were more immunogenic than unstressed control. Thus, our data strongly support the hypothesis that dimerization is not sufficient to increase the risk of ADA response. This makes immunologically sense, as to our knowledge there is no evidence that native IgA (dimeric) or IgM (pentameric) is more immunogenic than (monomeric) IgG, although head-to-head comparisons are lacking. In contrast, the immunogenicity of our positive control (submicron size aggregates) is in qualitative alignment with the vast literature about nanoparticulate antigens, which in general are much more immunogenic than antigens free in solution.[31,32] Interestingly, in our hands, even UV-irradiated dimers were not able to trigger ADA formation. This difference between our and Bessa's results could be explained by differences between the proteins, mouse models and treatment regimens used, or the extent of chemical modifications or combination of all those factors. It has been shown that the choice of mouse model and treatment regimen significantly influences the ADA production.[7,33,34] Our data show lack of ADA formation upon administration of dimers, but a clear response to submicron-size aggregates. These results indicate that dimers, even chemically modified ones, may be of lower ADA formation risk than submicron particles composed of chemically unmodified mIgG1. This suggests that aggregate size by itself might be a relevant factor influencing the immunogenicity risk, in line with the conclusion of earlier studies.[6,7,11-13]

Because dimers are a significant type of mAb aggregates present in commercially available products, insight into the potential immunogenicity of dimers is highly relevant from a clinical point of view. According to data presented in this article, dimerization does not appear to increase the risk of ADA formation.

References

1. Goswami S, Wang W, Arakawa T, Ohtake S. Developments and challenges for mAb-based therapeutics. *Antibodies*. 2013;2:452-500.
2. Narhi LO, Schmit J, Bechtold-Peters K, Sharma D. Classification of protein aggregates1. *J Pharm Sci*. 2012;101:493-498.
3. Mahler H, Friess W, Grauschopf U, Kiese S. Protein aggregation : pathways, induction factors and analysis. *J Pharm Sci*. 2009;98:2909-2934.
4. Ratanji KD, Derrick JP, Dearman RJ, Kimber I. Immunogenicity of therapeutic proteins: influence of aggregation. *J Immunotoxicol*. 2014;11:99-109.
5. Filipe V, Jiskoot W, Basmeleh AH, Halim A, Schellekens H, Brinks V. Immunogenicity of different stressed IgG monoclonal antibody formulations in immune tolerant transgenic mice. *MAbs*. 2012;4:740-752.
6. Bessa J, Boeckle S, Beck H, et al. The immunogenicity of antibody aggregates in a novel transgenic mouse model. *Pharm Res*. 2015;32:2344-2359.
7. Freitag AJ, Shomali M, Michalakis S, et al. Investigation of the immunogenicity of different types of aggregates of a murine monoclonal antibody in mice. *Pharm Res*. 2015;32:430-444.
8. van Beers MMC, Sauerborn M, Gilli F, Brinks V, Schellekens H, Jiskoot W. Oxidized and aggregated recombinant human interferon beta is immunogenic in human interferon beta transgenic mice. *Pharm Res*. 2011;28:2393-2402.
9. Chirmule N, Jawa V, Meibohm B. Immunogenicity to therapeutic proteins: impact on PK/PD and efficacy. *AAPS J*. 2012;14:296-302.
10. Moussa EM, Panchal JP, Moorthy BS, et al. Immunogenicity of therapeutic protein aggregates. *J Pharm Sci*. 2016;105:417-430.
11. Telikepalli S, Shinogle HE, Thapa PS, et al. Physical characterization and in vitro biological impact of highly aggregated antibodies separated into size-enriched populations by fluorescence-activated cell sorting. *J Pharm Sci*. 2015;104:1575-1591.
12. Fathallah AM, Chiang M, Mishra A, et al. The effect of small oligomeric protein aggregates on the immunogenicity of intravenous and subcutaneous administered antibodies. *J Pharm Sci*. 2015;104:3691-3702.
13. Kijanka G, Bee JS, Korman SA, et al. Submicron size particles of a murine monoclonal antibody are more immunogenic than soluble oligomers or micron size particles upon subcutaneous administration in mice. *J Pharm Sci*. 2018;107(11):2847-2859.
14. Jiskoot W, Kijanka G, Randolph TW, et al. Mouse models for assessing protein immunogenicity: lessons and challenges. *J Pharm Sci*. 2016;105:1567-1575.
15. Remmele RL, Callahan WJ, Krishnan S, et al. Active dimer of epratuzumab provides insight into the complex nature of an antibody aggregate. *J Pharm Sci*. 2006;95:126-145.
16. Iwura T, Fukuda J, Yamazaki K, Kanamaru S, Arisaka F. Intermolecular interactions and conformation of antibody dimers present in IgG1 biopharmaceuticals. *J Biochem*. 2014;155:63-71.
17. Iacob RE, Bou-Assaf GM, Makowski L, Engen JR, Berkowitz SA, Houde D. Investigating monoclonal antibody aggregation using a combination of H/DX-MS and other biophysical measurements. *J Pharm Sci*. 2013;102:4315-4329.
18. US Pharmacopeia. *USP/NF general chapter <85>, Bacterial Endotoxins Test. In: US Pharmacopeia, NationalFormulary, USP 38*. Rockville, MD: United States Pharmacopeial Convention; 2015.
19. Filipe V, Kükrer B, Hawe A, Jiskoot W. Transient molten globules and metastable Aggregates induced by brief exposure of a monoclonal IgG to low pH. *J Pharm Sci*. 2012;101:2327-2339.
20. Kelly SM, Jess TJ, Price NC. How to study proteins by circular dichroism. *Biochim Biophys Acta*. 2005;1751:119-139.
21. Barnard JG, Singh S, Randolph TW, Carpenter JF. Subvisible particle counting provides a sensitive method of detecting and quantifying aggregation of monoclonal antibody caused by freeze-thawing: insights into the roles of particles in the protein aggregation pathway. *J Pharm Sci*. 2011;100:492-503.
22. Kijanka G, Bee JS, Bishop SM, Que I, Löwik C, Jiskoot W. Fate of multimeric oligomers, submicron, and micron size aggregates of monoclonal antibodies upon subcutaneous injection in mice. *J Pharm Sci*. 2016;105:1693-1704.
23. Filipe V, Que I, Carpenter JF, Löwik C, Jiskoot W. In vivo fluorescence imaging of IgG1 aggregates after subcutaneous and intravenous injection in mice. *Pharm Res*. 2014;31:216-227.
24. Qiu ZJ, Ying Y, Fox M, et al. A novel homogeneous biotin-digoxigenin based assay for the detection of human anti-therapeutic antibodies in autoimmune serum. *J Immunol Methods*. 2010;362:101-111.
25. Vermeer AWP, Bremer MGEG, Norde W. Structural changes of IgG induced by heat treatment and by adsorption onto a hydrophobic teflon surface studied by circular dichroism spectroscopy. *Biochim Biophys Acta*. 1998;1425:1-12.
26. Greenfield NJ. Using circular dichroism spectra to estimate protein secondary structure. *Nat Protoc*. 2007;1:2876-2890.
27. Yang J, Goetze AM, Flynn GC. Assessment of naturally occurring covalent and total dimer levels in human IgG1 and IgG2. *Mol Immunol*. 2014;58:108-115.
28. Paul R, Graff-Meyer A, Stahlberg H, et al. Structure and function of purified monoclonal antibody dimers induced by different stress conditions. *Pharm Res*. 2012;29:2047-2059.
29. Plath F, Ringler P, Graff-Meyer A, et al. Characterization of mAb dimers reveals predominant dimer forms common in therapeutic mAbs. *MAbs*. 2016;8:928-940.
30. Adem YT, Molina P, Liu H, Patapoff TW, Sreedhara A, Esue O. Hexyl glucoside and hexyl maltoside inhibit light-induced oxidation of tryptophan. *J Pharm Sci*. 2014;103:409-416.
31. Gregory AE, Titball R, Williamson D. Vaccine delivery using nanoparticles. *Front Cell Infect Microbiol*. 2013;3:1-13.
32. Benne N, van Duijn J, Kuiper J, Jiskoot W, Slütter B. Orchestrating immune responses: how size, shape and rigidity affect the immunogenicity of particulate vaccines. *J Control Release*. 2016;234:124-134.
33. Kijanka G, Jiskoot W, Schellekens H, Brinks V. Effect of treatment regimen on the immunogenicity of human interferon beta in immune tolerant mice. *Pharm Res*. 2013;30:1553-1560.
34. van Beers MMC, Sauerborn M, Gilli F, et al. Hybrid transgenic immune tolerant mouse model for assessing the breaking of B ell tolerance by human interferon beta. *J Immunol Methods*. 2010;352:32-37.